Single Image Dehazing using Extended Local Dark Channel Prior

Pulkit Dwivedi (pdwivedi1990@gmail.com)
Soumendu Chakraborty
Indian Institute of Information Technology

Research Article

Keywords: Image dehazing, atmospheric scattering model, transmission estimate, dark channel prior

Posted Date: December 21st, 2022

DOI: https://doi.org/10.21203/rs.3.rs-2387969/v1

Additional Declarations: No competing interests reported.

Single Image Dehazing using Extended Local Dark Channel Prior

Pulkit Dwivedi[1] and Dr Soumendu Chakraborty[1]

[1]Department of Computer Science, Indian Institute of Information Technology, Lucknow, India.

Contributing authors: pdwivedi1990@gmail.com; soum.uit@gmail.com;

Abstract

Image dehazing is an important technique aimed at eliminating the haze in the atmosphere to enhance the image's visual quality. There are many applications where it has been used as a prepossessing step, such as in event detection. In recent years, the dark channel prior methodology has been recognised as an effective approach for eliminating haze from hazy images. However, the main drawback of the existing dark channel prior methodology is that it only considers a single color channel of the RGB image with pixels having minimum intensity values. This non-uniform selection of the dark channel from a single channel eradicates the effect of the transmission across the different channels of the hazy image. Hence, the haze cannot be removed to a great extent using the existing method. So, here we propose an approach where the dark channel will be computed from all three channels of an image by selecting the minimum intensity. The main advantage of using the proposed prior-based methodology for image dehazing over deep neural network-based models such as CNN or GANs is that training deep models requires a large amount of training data, thus resulting in a longer training time. Experimental outcomes exhibit that the proposed technique outperforms state-of-the-art methods on synthetic datasets as well as real-world hazy images. The findings demonstrate that the proposed technique obtains better accuracy as compared to the state-of-the-art methods and recent deep learning-based models over the D-HAZY, I-HAZE, and O-HAZE databases.

Keywords: Image dehazing, atmospheric scattering model, transmission estimate, dark channel prior

1 Introduction

Due to poor climatic environment like fog, smoke, smog, mist, or dust, the effects of particles in the atmosphere have a significant impact on the image quality. It degrades to a great extent. The light gets dispersed in various directions when it strikes these atmospheric particles. This results in images that are faded in color and have low contrast. Image luminance also gets scattered. Due to this, human vision and some outdoor computer vision systems have difficulty identifying an object's characteristics. The main challenge in the dehazing process is due to the different densities of haze across different regions of a hazy image. As a result, eliminating haze from an image is a complex task, and in computer vision applications, this is a tremendously desired technology. Image dehazing techniques have been advantageous in numerous applications in the real world. These include satellite imagery systems where small details need to be detected to create accurate maps. It also has a significant contribution in military systems where the quality of the image deteriorates in extremely cold border areas due to the presence of snow. Apart from these, it can also be applied to underwater imaging where maintenance of underwater structures such as pipelines or cables is required. Other areas of application include video-assisted transportation, outdoor video monitoring, remote sensing photography assessment, fracture detection in medicine, image deraining [1] [2] etc.

Since haze, smog, or smoke cause impediments for computer vision systems, a significant and fast expanding group is devoted for eliminating the haze and its effects from digital images. Thus, numerous methodologies are available for dehazing the hazy images. The most successful methods of image dehazing [3], [4], [5], [6] are majorly established on the atmospheric scattering model put forward by McCartney [7] according to which a hazy image formed as shown in Fig. 1 can be defined as follows:

$$I(x) = J(x)t(x) + A(1 - t(x)) \tag{1}$$

where x represents the image coordinates, I represents the observed hazy image, J represents the haze-free image, A represents the global atmospheric light, and t represents the transmission map. The transmission, $t(x)$, estimates the proportion of light that enters the camera but is not dispersed by the atmosphere. The transmission value for an object far away from the camera will be lower, while the transmission value for a nearby object will be closer to one.

The major aim of image dehazing process is to retrieve haze free image, J , from a hazy image, I. Once A and t are estimated from I, J can be mathematically calculated as:

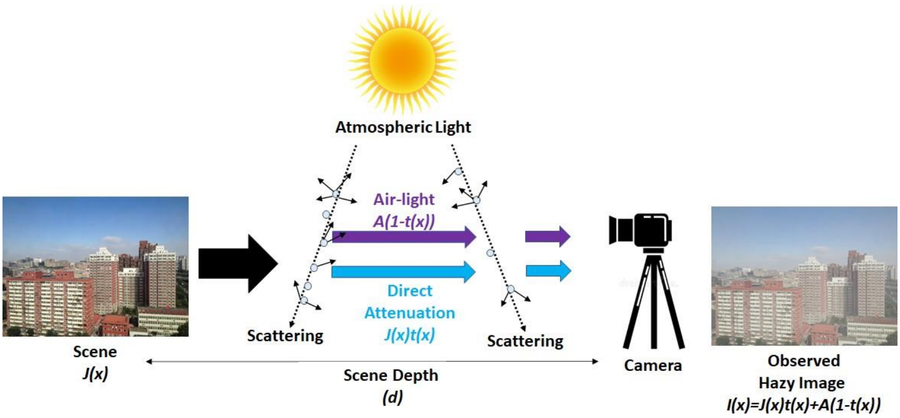

Fig. 1 Formation of the hazy image

$$J(x) = \frac{I(x) - A}{t(x)} + A \tag{2}$$

Various remarkable advancements in the field of image dehazing have been seen in recent years. These methods are typically based on chromatic, textural, and contrast properties. Among conventional algorithms for image dehazing, the dark channel prior (DCP) [8] is widely recognized. It is a novel technique that has been developed to overcome the limitations of many previous approaches. It was inspired by an earlier haze removal method known as the dark object subtraction technique [9]. The dark channel prior (DCP) is a common pattern in haze-free images. It has been observed that the hazy image's dark pixels, i.e., the pixels that receive immensely low intensity values, provide a definite estimation of the transmission of the haze.

However, in most non-sky patches of the haze-free image, DCP considers one color channel of a RGB image that consists of a few pixels having minimum intensity. This leads to non-uniform selection of the dark channel and, thus, leaves some amount of haze in the image. In this paper, we propose an improved methodology that extends the existing single-channel DCP technique to a multi-channel approach. This proposed method considers all three channels of an image to calculate the dark channel. We have also evaluated our methodology on the indoor and outdoor hazy image databases. The experiment results show that our improved model achieves the highest PSNR as well as SSIM values as compared to the state-of-the-art algorithms and recent deep learning based methods.

The remaining paper is organised as follows: Section 2 presents the related work in the field of image dehazing; Section 3 is devoted to existing image dehazing methodology using dark channel prior; Section 4 illustrates proposed methodology; Section 5 is devoted to experimental results in terms of the quality measures used, datasets used, comparison with the deep learning based method as well as state-of-the-art methods and parameter tuning; and finally, the conclusions are drawn in Section 6.

2 Related Work

A crucial task in computer vision and image processing systems is to improve and enhance the image. Many methods and strategies have emerged to repair hazy images. Tarel and Hautiere [10] presented the first single image dehazing approach. The method makes use of a filtering technique to eliminate haze from the images. Here, the value of transmission is estimated as a percentage of the difference between the local average and the local standard deviation of an image. An extended version of the median filter is applied to further improve the transmission. The method is suitable for images generated using white balancing as a preprocessing step. He et al. [8] introduced a novel methodology which is established on dark channel prior. According to this approach, there should be at least one dark color channel that contains pixels with very low intensities. This analysis is valuable for estimating haze depth and restoring a dehazed image of good quality. Meng et al. [11] extended the dark channel prior. To prevent image distortion across sharp corners, it constructs an optimization function which combines the constraints that were present due to scene radiance with a weighted L1-norm dependent contextual regularization. Sharma et al. [12] proposed a method that uses a type-2 membership function based similarity function matrix. This method also estimates the depth map of the hazy image along with the global atmospheric light and finally uses (1) to remove the haze. Zhang et al. [13] proposed a methodology in which a hazy image is segregated into multiple regions having different haze densities. Here, global atmospheric light is replaced by estimating the local atmospheric light in each region. This method uses the dark channel prior in order to estimate the transmission. In this approach, they implemented an iterative method and imposed a termination condition. According to the algorithm, the iteration should be suspended whenever a given condition is met. The parameter value used in the termination criteria is estimated purely based on the experiments. This method requires choosing the parameter value based on the input hazy image. This means that the same parameter value cannot be fixed for every kind of hazy image, and the main drawback of this methodology is that it is highly dependent on choosing an accurate parameter value. Fattal [6] proposed an algorithm that is established on the concept of estimating the optical transmission that eradicates the diffusion of light and restores the contrast of an image, resulting in highly visible images. It is based on the analysis that the pixels in small image patches usually have a one-dimensional RGB color space distribution known as color lines. As haze causes color lines to drift from the RGB origin, we can estimate the transmission map by measuring the lines offset from the origin. This strategy comes up short in non-homogeneous and dense fog regions. Ancuti et al. [14] proposed a technique to estimate local airlight for dehazing hazy images that was used in the multi-scale fusion technique. The method was created to address issues related to the scattering effect, which is particularly noticeable in hazy nighttime scenes. The method is, however, suitable for day-time hazy scene enhancement. Gao et al. [15] proposed a dual-fusion technique for dehazing a single image. In this method, the sky and non-sky portions are acquired by a segmentation approach that divides the image into two halves. For a single image smooth, a multi-region fusion approach is proposed in order to adequately optimise the transmission. The brightness transform function builds an exposure fusion technique to efficiently eliminate haze from the image.

In recent years, various deep learning approaches have been widely implemented in major fields of computer vision. Some attempts have also been made for haze removal as well. Cai et al. [16] proposed a method using convolutional neural networks (CNNs) that uses CNN layers to extract the features that are accountable for producing haze in an image. This method uses the Middlebury stereo dataset to train the neural network. The approach uses a non-linear activation function with a bilateral restraint to optimise convergence. Ren et al. [17] uses a multi-scale CNN to specifically determine the transmission map from hazy images. The training was done with synthetically produced hazy images, which were acquired from the images without any haze, and their related depth maps, which were used to implement a generalised light propagation model. Dudhane et al. [18] proposed the LIGHT-Net dehazing model that consists of two modules. In this approach, they used one module to eliminate the color cast and to maintain the color constancy. Another module is used to reduce haze, which is built using an inception-residual block. AOD-Net [19] proposed a system for dehazing an image where a convolutional neural network is used to determine the haze-free image. In this method, estimating the transmission map is not required. CycleDehaze [20] is a technique for image dehazing that does not require hazy and equivalent images of ground truth for training. This method improves on CycleGAN [21], which uses cycle consistency loss and perceptual loss to produce more visually appealing and realistic haze-free images. Chen et al. [22] proposed a model with a super-resolution approach and a knowledge transfer method inspired by the Knowledge Transfer Dehazing Network (KTDN) [23] and Trident Dehazing Network (TDN) [24]. This deep neural network is made up of a teacher network, a dehaze network, and a super-resolution network. This method creates low-level feature maps using the teacher network. To gather the data required for image restoration, the teacher network is trained using ground truth pairs from the dataset. While some current CNN-based techniques are quite efficient in eliminating homogeneous haze, they are not reliable in non-homogeneous situations. There are primarily two factors for this. First, the dehazing method is prone to losing texture details because of the complex haze distribution. Second, training with limited data results in over-fitting as training pairs are difficult to gather. Fu et al. [25] proposed a new dehazing network, DW-GAN, that employs the 2D discrete wavelet transform (DWT). To address these two problems, the authors put forward a two-branch architecture. This strategy maintains more high-frequency information in feature maps by employing wavelet transform in the DWT branch. In the knowledge adaption branch, ImageNet [26] pre-trained Res2Net [27] is used to avoid over-fitting. Finally, the artefacts in the dehazed images are reduced using a patch-based discriminator. Liu et al. [28] propose the PBGAN model. This model is comprised of two GAN modules. One module is used to enhance the contrast, while another module is used to enhance the texture of the hazy image. An inversion-adversarial loss and an inversion-cycle consistency loss are introduced to train the generator in order to enhance the contrast. Two CNNs are used to learn the ambient light coefficient and the transmission map, respectively, to enhance the texture of the hazy image.

3 Image dehazing using dark channel prior

The dark channel prior based image dehazing method was first proposed by He et al. in [8]. This technique for removing haze is established on the key observation that within an image patch, there exist a few pixels that have an intensity value near zero for at least one color channel. When the intensity tends to zero, the color diverges towards dark or black. That's why this phenomenon is called "the dark channel." Based on this, the dark channel, J^{dark}, of a haze free image J is written as:

$$J^{dark}(x) = \min_{y \in \Omega(x)} \left(\min_{c \in \{r,g,b\}} J^c(y) \right) \tag{3}$$

where J^c is the color channel $c \in \{r, g, b\}$ of J and $\Omega(x)$ is the local patch centred at x.

Based on the concept of a dark channel, J's dark channel is low in intensity, with the exception of the sky region, and tends to be zero [8].

$$J^{Dark} \rightarrow 0$$

This phenomenon is referred to as the "dark channel prior." Pixels whose values are distant from zero are generated by the dark channels in hazy images. Global atmospheric light is generally vivid, and in the local patch, the three color channel's minimum value is greatly increased by combining airlight and direct attenuation. As a result, it's reasonable to conclude that the dark channel's pixel values can be used to estimate haze intensity [8].

In the dark channel prior dehazing technique, the dark channel is initially formulated from the hazy input image as shown in (3)[8]. Later, from the dark channel, the atmospheric light and the transmission map is computed. The refinement of the transmission map is done and the dehazed image is constructed as shown in (2)[8].

After dividing both sides of (1) by A^c, the minimum intensity in the local patch of each color channel is determined mathematically as follows:

$$\min_{y\in\Omega(x)} \frac{I^c(y)}{A^c} = \tilde{t}(x) \min_{y\in\Omega(x)} \frac{J^c(y)}{A^c} + 1 - \tilde{t}(x) \tag{4}$$

The transmission in the local patch $\Omega(x)$ is considered to be constant here and denoted by $\tilde{t}(x)$. The three color channels' min operator can be applied to (4) as below:

$$\min_{y\in\Omega(x)} (\min_c \frac{I^c(y)}{A^c}) = \tilde{t}(x) \min_{y\in\Omega(x)} (\min_c \frac{J^c(y)}{A^c}) + 1 - \tilde{t}(x) \tag{5}$$

As J is haze free image, the dark channel of haze free image is near to zero due to dark channel prior. Thus,

$$J^{Dark}(x) = \min_{y\in\Omega(x)} (\min_c J^c(y)) = 0$$

As A^c always positive,

$$J^{Dark}(x) = \min_{y\in\Omega(x)} (\min_c \frac{J^c(y)}{A^c}) = 0 \tag{6}$$

Substituting this in (5),

$$\tilde{t}(x) = 1 - \min_{y\in\Omega(x)} (\min_c \frac{I^c(y)}{A^c}) \tag{7}$$

Now, if all of the haze is removed from the image, it will not appear natural, and the sense of depth will be loosened. Hence, a very minute proportion of haze is kept for the far objects by presenting a constant parameter, Ω which ranges between [0,1] into (7).

$$\tilde{t}(x) = 1 - \Omega \min_{y\in\Omega(x)} (\min_c \frac{I^c(y)}{A^c}) \tag{8}$$

The atmospheric light, A, must be estimated in order to obtain the transmission map, $\tilde{t}(x)$. Thus, for that, 0.1% of the dark channel's brightest pixels are chosen, and then the color with the maximum intensity of the chosen pixels is taken as the value for atmospheric light. Also, it is further required to smoothen the transmission map so that it does not lead to false textures and blocking artifacts. Thus, soft matting is applied for this purpose [8].

The image can be dehazed and the scene radiance can be revived as given in (1) with the help of the atmospheric light and the transmission map. When the transmission term, $t(x)$, is close to zero, the direct attenuation term, $J(x)t(x)$, is almost non-existent. As a result, a lower bound, t_0, is applied to the transmission t(x), allowing some haze to be preserved in densely hazy areas. The final haze free image $J(x)$ can be retrieved as follows:

$$J(x) = \frac{I(x) - A}{max(t(x), t_0)} + A \tag{9}$$

Like other dehazing methods, dark channel prior has few drawbacks as well. It fails to estimate the transmission when the entities in the image are constitutionally like the atmospheric light and are not covered by shadows. It fails to recover the image when the sky area is huge or there is a large white area in the scene. Since DCP is a physics-based method, it also fails when the haze model in (1) is physically invalid. The dark channel prior even fails to recover the image under non-homogeneous haze or when the haze is too dense.

4 Proposed Methodology

The main drawback of the existing dark channel prior methodology is that it does not uniformly select the dark channel due to which the effect of transmission is eliminated across all the color channels of a hazy image. Here, the dark channel is computed while considering the single color channel of a RGB hazy image that has pixels with minimum intensity. We propose a methodology where the dark channel is computed considering all three channels of an image by selecting the minimum intensity. These individual dark channels will be used to compute the individual transmission maps of each color channel. Thus, using (6), the dark channel of the red color channel is given by

$$J_r^{dark}(x) = \min_{y \in \Omega(x)} (\min_r J^r(y)) \tag{10}$$

where J^r is the red color channel of J.

Similarly, the dark channel of the green and blue color channels is given by

$$J_g^{dark}(x) = \min_{y \in \Omega(x)} (\min_r J^g(y)) \tag{11}$$

$$J_b^{dark}(x) = \min_{y \in \Omega(x)} (\min_r J^b(y)) \tag{12}$$

where J^g and J^b is the green and blue color channel of J respectively.

Hence, from (10), (11) and (12), it can be seen that in the proposed methodology we are computing the individual dark channels for each color channel of a hazy image, as compared to (6) where the dark channel is calculated considering a single color channel of an image with pixels having minimum intensity values. This is the principal novelty of the proposed methodology. After computing the individual dark channels of an image, the individual transmission maps are calculated. Thus, using (10), (11), (12) and (8), we calculate the transmission maps for each color channel. Therefore, the transmission for the red color channel is given by

$$\tilde{t}_r(x) = 1 - \Omega \min_{y \in \Omega(x)} (\min_{r} \frac{I^r(y)}{A^c}) \tag{13}$$

Similarly, transmission for green and blue color channel is calculated as

$$\tilde{t}_g(x) = 1 - \Omega \min_{y \in \Omega(x)} (\min_{g} \frac{I^g(y)}{A^c}) \tag{14}$$

$$\tilde{t}_b(x) = 1 - \Omega \min_{y \in \Omega(x)} (\min_{b} \frac{I^b(y)}{A^c}) \tag{15}$$

In (13), (14) and (15) it can be seen that we are computing the individual transmission maps for each color channel, whereas in the existing dark channel prior approach, it is computed using the dark channel for a single channel, as shown in (8). This uniform selection of the dark channel in the proposed methodology considers the effect of the transmission across the different channels of the hazy image and helps to eliminate the haze in a better way as compared to the existing dark channel prior method. The final transmission in the local patch is calculated as the mean transmission of all the three color channels using (13), (14), (15)

$$\tilde{t}_{avg}(x) = (\tilde{t}_r(x) + \tilde{t}_g(x) + \tilde{t}_b(x))/3 \tag{16}$$

We estimate the transmission using the above mathematical formula. This means that the average transmission considers each color channel and helps to remove the haze from an image to a great extent. Now, this above calculated value of transmission can be used to compute the final scene radiance. The final scene radiance is written as

$$J(x) = \frac{I(x) - A}{max(t_{avg}(x),\ t_0)} + A \tag{17}$$

where $t_{avg}(x)$ is the proposed transmission map and t_0 is the lower bound applied to this transmission value.

The overall workflow of the proposed methodology is shown in Fig. 2, which illustrates that the proposed model is applied to a hazy image to compute the corresponding dark channels across each color channel. Atmospheric light is computed by taking 0.1% of the brightest pixels in the dark channel. Using the individual dark channels of the hazy image and the atmospheric light, the corresponding transmission map of each channel is computed for each color channel. A mean transmission map is then computed, and it is refined using a guided filter. This mean refined transmission map is then used to generate the final haze-free image.

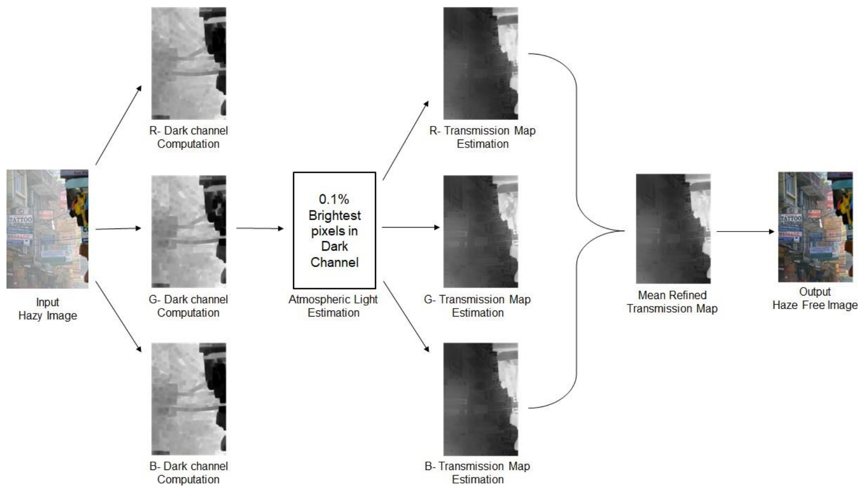

Fig. 2 Flow diagram of the proposed methodology.

When the value of the transmission is close to 1, it signifies that the dehazing is done in an efficient way. In order to compare the values of the transmission map, we take a 10x10 block of the transmission map of the image dehazed using the dark channel prior as well as the proposed methodology. We considered one hazy indoor image from the D-HAZY Middlebury dataset [29] and one outdoor image from the O-HAZE [30] dataset. It can be seen from Fig. 3 that the pixels of the transmission map are closer to 1 when the image is dehazed using the proposed methodology as compared to when it is dehazed using the dark channel prior. The final transmission achieved by the proposed methodology is closer to 1 than the transmission obtained by the dark channel prior method for indoor as well as outdoor images. This indicates that the proposed method enhances the transmission's accuracy and thus results in better dehazed images.

In order to prove the effectiveness of the proposed methodology, we performed a pixel level comparison using two hazy images from the D-HAZY

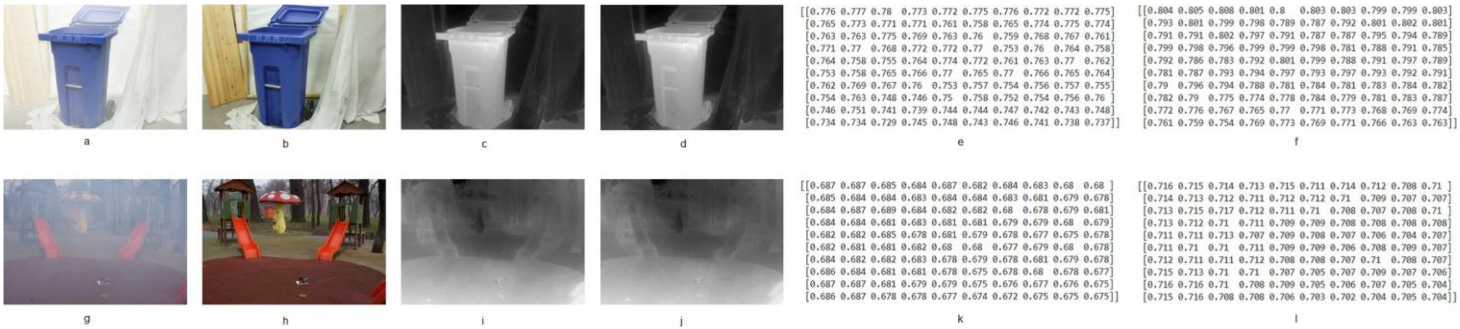

Fig. 3 Transmission Map Comparison :(a) and (g): Hazy Image, (b) and (h): Ground Truth Image, (c) and (i): Transmission map using Dark Channel Prior, (d) and (j): Transmission map using proposed methodology, (e) and (k): 10x10 block of transmission map using dark channel prior, (f) and (l): 10x10 block of transmission map using proposed methodology

Middlebury dataset [29]. A 10x10 block of each image is taken and we compare the pixels of all the three color channels of the RGB image using the dark channel prior method and the proposed methodology. It can be seen in Fig. 4 that the pixels of the dehazed image using the proposed methodology are significantly more closer to the pixels of the ground truth image as compared to the dark channel prior method. This can be observed across all the three color channels of the dehazed image. We also highlighted some pixels in each color channel that are highly close to the ground truth image while dehazing the image using the proposed method. It can be seen that the proposed method is more effective at eliminating the haze from a hazy image as compared to the dark channel prior method.

We also plot the absolute pixel difference (APD) between the ground truth image and the image dehazed using the dark channel prior as well as the proposed methodology for each color channel. This absolute pixel difference plot is less sensitive to subtle shifts and is an excellent metric for image similarity detection. It acts as a robust image correlation metric by identifying changes in the image pixels between the ground truth image and the dehazed image. For this analysis, we considered three indoor images from the D-HAZY Middlebury dataset [29] and two outdoor images from the O-HAZE [30] dataset. We have also resized the images in order to better visualise the graphs. The red plot in Fig. 5 shows the absolute pixel difference between the ground truth and the dark channel prior method, while the green plot shows the absolute pixel difference between the ground truth image and the proposed method. It can be seen that the peaks of the red plot are notably higher as compared to the green plot for each color channel. This can be observed in both indoor and outdoor images. Fig. 5 also shows the sum of the absolute pixel difference (APD) of the dark channel prior and the proposed methodology. In Fig. 5(c), the sum of APD between the ground truth image and the image dehazed using the dark channel prior for red color channel is 15604. When the same hazy image is dehazed using the proposed methodology, the sum of APD is reduced to 13960. In other images also, for each color channel, the sum of APD of the dark channel prior is significantly higher than the sum of APD of the proposed methodology. Hence, it can be inferred that the proposed methodology performs the dehazing task exceptionally well as compared to the existing dark channel prior method for both indoor and outdoor images.

The following are the major contributions of this method:

- We propose an approach for image dehazing using an extended local dark channel prior where we considered all the three color channels of a hazy image to compute the individual dark channel.
- Using the individual dark channels for each of the color channels, we computed the corresponding transmission maps and then used the mean transmission map to calculate the final haze free image.

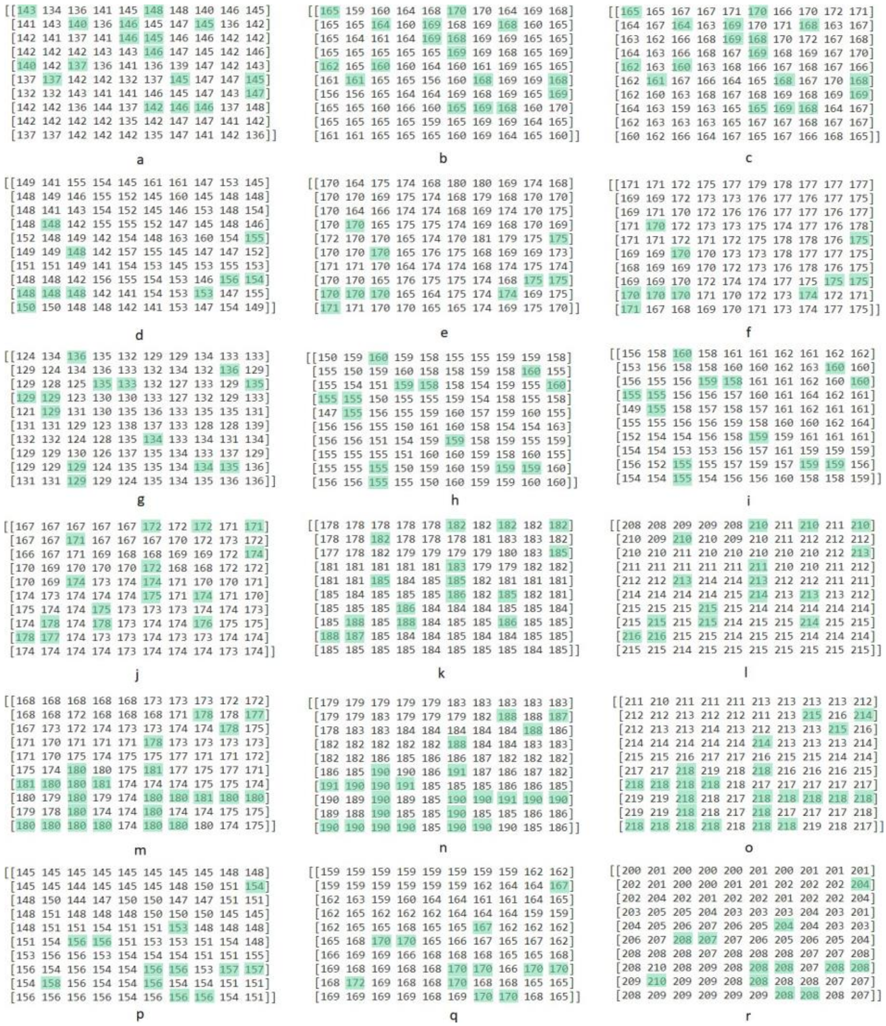

Fig. 4 Pixel level comparison of dark channel prior and the proposed methodology:
(a), (d), (g): r, g, b channels of 10x10 block of dehazed image -1 using dark channel prior
(b), (e), (h): r, g, b channels of 10x10 block of dehazed image -1 using proposed methodology
(c), (f), (i): r, g, b channels of 10x10 block of ground truth image -1
(j), (m), (p): r, g, b channels of 10x10 block of dehazed image -2 using dark channel prior
(k), (n), (q): r, g, b channels of 10x10 block of dehazed image -2 using proposed methodology
(l), (o), (r): r, g, b channels of 10x10 block of ground truth image -2

- The existing dark channel prior method tries to remove the transmission effect across all the channels using a common dark channel. As the transmission will be different across different channels, individual dark channels need to be considered.
- As we are uniformly selecting the dark channel from all three color channels, this will take into account the effect of transmission across different channels

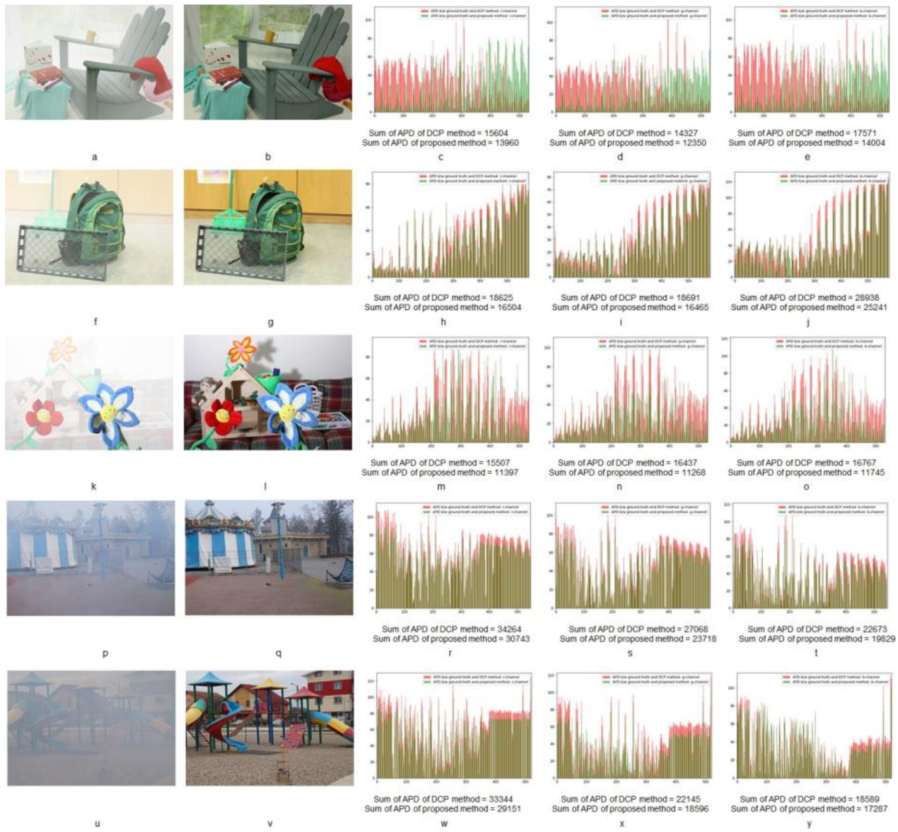

Fig. 5 Absolute pixel difference (APD) plot for ground truth and dehazed image using DCP and proposed methodology
(a) , (f), (k), (p), (u): Hazy images
(b) , (g), (l), (q), (v): Ground truth images
(c) , (h), (m), (r), (w): Absolute pixel difference between ground truth and dehazed image using DCP and proposed method for red channel
(d) , (i), (n), (s), (x): Absolute pixel difference between ground truth and dehazed image using DCP and proposed method for green channel
(e) , (j), (o), (t), (y): Absolute pixel difference between ground truth and dehazed image using DCP and proposed method for blue channel

of a hazy image, and thus, haze can be removed in a better way as compared to the existing dark channel prior method.

- We compare the transmission map of the dehazed image using the dark channel prior method and the proposed method. It can be seen that the transmission map of the image dehazed using the proposed methodology is closer to 1 as compared to that of the dark channel prior. This shows that the transmission accuracy has increased with the proposed methodology, thus increasing the overall image quality.
- We perform the pixel level analysis by taking a small block of the hazy image. We compare the pixel values of all the three color channels using the dark

channel prior method and the proposed methodology. It is observed that the pixels of the dehazed image using the proposed methodology are much closer to the ground truth image pixels as compared to the dark channel prior method.

- We also plot the absolute pixel difference in order to compare the proposed methodology with the dark channel prior. It can be seen that the absolute pixel difference (APD) between the ground truth image and the dehazed image using dark channel prior is remarkably higher than the proposed methodology.

5 Experimental Results

In order to assess the performance of the proposed methodology, we present the quantitative as well as qualitative evaluation results by demonstrating our dehazing results on several groups of hazy images. We analyse the performance of the proposed dehazing technique and compared it with the existing method of image dehazing using dark channel prior and other state-of-the-art methods, including some standard deep learning models.

5.1 Quality Measures

An extensive quantitative assessment is performed on the existing state-of-the-art dark channel prior single image dehazing method and the proposed method. We use two metrics to evaluate these dehazing methods: PSNR (Peak-Signal-to-Noise Ratio) and SSIM (Structural Similarity Index Measure) [31]. PSNR provides a pixel-wise evaluation and is capable of indicating the effectiveness of haze removal. The high PSNR value indicates that there is less noise in the image and the image has been restored well. It is the ratio of a signal's maximum possible value to the power of distorting noise that has an impact on the quality of its representation. It can be calculated as [32]

$$PSNR = 10 \times \log_{10}\left(\frac{L^2}{MSE}\right) \tag{18}$$

where

$$MSE = \frac{1}{mn}\sum_{i=0}^{m-1}\sum_{j=0}^{n-1}[y(i,j) - x(i,j)]^2$$

Here, x represents the generated image, y represents the really clear image, and the image size is $m \times n$. MSE represents the mean square error between x and y and L is the dynamic range of the pixel values.

SSIM is an image quality measure that is implemented to gauge the resemblance of two images where the mean is used to calculate the brightness, the standard deviation is used to calculate the contrast, and the covariance is used to calculate the structure similarity. It can be calculated as [33]

$$SSIM = \frac{(2\mu_x\mu_y + c_1)(2\sigma_{xy} + c_2)}{(\mu_x^2 + \mu_y^2 + c_1)(\sigma_x^2 + \sigma_y^2 + c_2)} \tag{19}$$

where μ_x and μ_y are the averages of x and y, σ_x^2 and σ_y^2 are the variances of x and y, σ_{xy} is the covariance of x and y. The constants $c_1 = (k_1L)^2$ and $c_2 = (k_2L)^2$ are used to maintain stability, and the default values are $k_1 = 0.01$ and $k_2 = 0.03$. The larger values of PSNR and SSIM indicate better dehazing and perceptual quality.

5.2 Datasets Used

In our experiment, we use the following datasets as hazy images and the original images as ground truth images.

- D-HAZY: A dataset to evaluate quantitatively dehazing algorithms. [34] - The main challenge presented by this dataset is that the images in it correspond to the indoor environment. Since these are indoor images, the color of the images appears to be dull with poor contrast.
- I-HAZE: A dehazing benchmark with real hazy and haze-free indoor images. [35] - Here also, the images are from the indoor domestic environment. The images are dull in color with low contrast, so eliminating haze is a challenging task for these types of images.
- O-HAZE: A dehazing benchmark with real hazy and haze-free outdoor images. [30] - The main challenge presented by this dataset is that the images are comprised of outdoor scenes which are affected by cloudy weather, sunset/sunrise haze, wind speed, etc.

5.3 Comparison with DCP and other state-of-the-art image dehazing methods

To recover the hazy images, different types of images from the above datasets are used. Each of the images taken is dehazed using the state-of-the-art method as well as the proposed method. Each dehazed image is then compared with its ground truth image, and then PSNR and SSIM values are computed. Extensive experiments resulted in the conclusion that our method performed best on synthetic indoor and outdoor hazy images.

5.3.1 Comparison using D-HAZY Dataset

The D-HAZY dataset is based on the Middlebury [29] and NYU Depth [36] datasets that contain over 1400 complex scene images and their related depth maps. It includes high-resolution real-world images, with the depth maps from each scene being used to create synthetic hazy images. Fig. 6 shows four images from the D-HAZY dataset [34] which have been restored using the dark channel prior based method and the proposed method. According to the study results of the experiments, the existing dark channel prior based dehazing method does not provide satisfactory results for removing the haze, while the proposed methodology achieves more satisfactory results. Besides, the proposed method obtains the highest PSNR and SSIM for the restored images compared to the DCP method, so the restored images using this method are even closer to the ground truth. Therefore, since the PNSR and SSIM values are high, it can be concluded that there is less noise in the dehazed image. It can be observed from Fig. 6 (c) that there is an increase of 2.041 dB in the PSNR and 0.048 in the SSIM, which indicates that the proposed methodology is more proficient at eliminating the haze and reconstructing the image to its original quality.

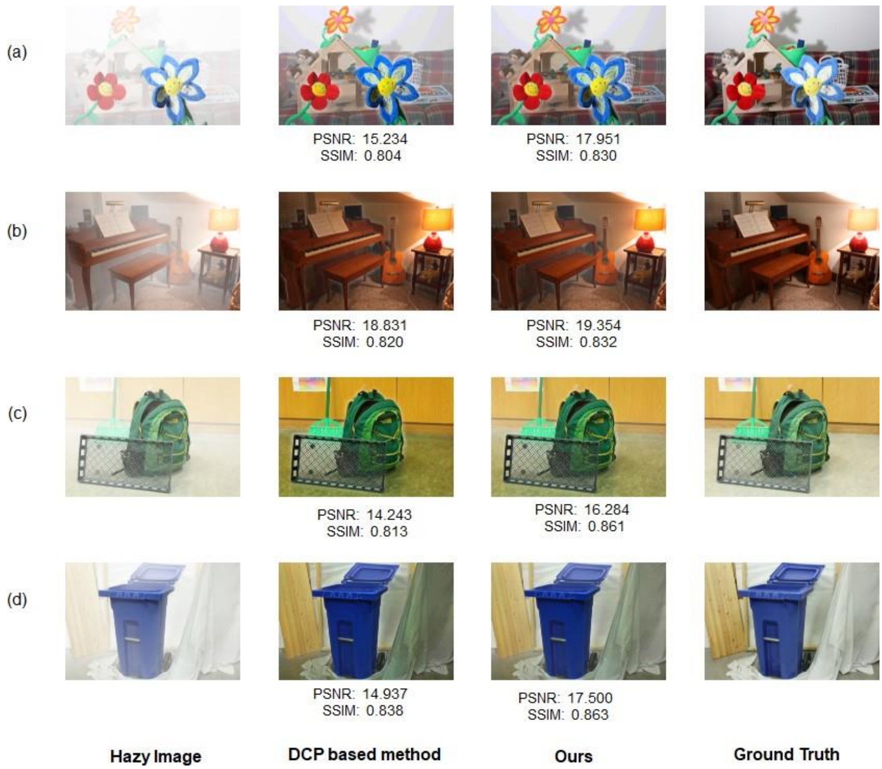

Fig. 6 Comparison of the restored images using DCP and proposed methodology

We also compare the image quality measures by considering three image resolutions, i.e. 128×96, 640×480, and 1024×768 for each dataset.

In Fig. 7 we compare the PSNR and SSIM of Dark Channel Prior with the proposed methodology for the D-HAZY Middlebury dataset. It can be seen that, for low resolution images (128×96), there is a slight increase in the PSNR value, but for higher resolution images (640×480 and 1024×768), there is a significant increase in the PSNR and SSIM values. The highest SSIM of 0.88 is obtained for 1024×768 resolution images.

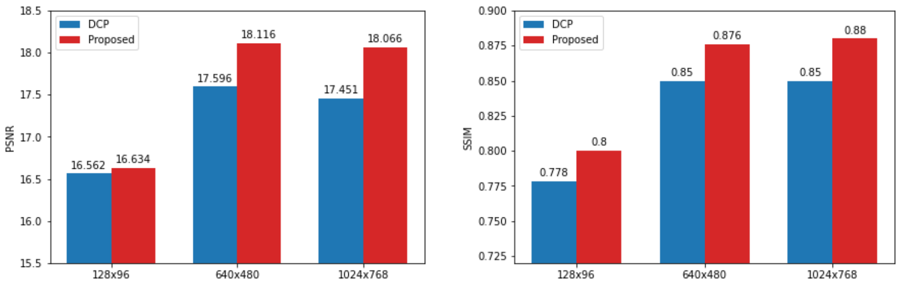

Fig. 7 PSNR and SSIM comparison of Dark Channel Prior and proposed methodology of D-HAZY Middlebury Dataset

A similar analysis is done on the D-HAZY NYU dataset. The default resolution of the D-HAZY NYU dataset is 640×480, so the PSNR for this image resolution is high as compared to other image resolutions. It can be seen from Fig. 8 that the proposed method has performed well. There is an increase in the PSNR and SSIM values for all the image resolutions.

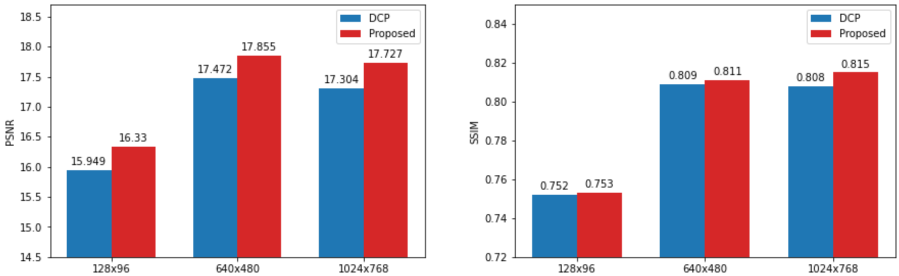

Fig. 8 PSNR and SSIM comparison of Dark Channel Prior and proposed methodology of D-HAZY NYU Dataset

5.3.2 Comparison using I-HAZE Dataset

The I-HAZE dataset [35] comprises of 35 indoor images that are hazy and their corresponding ground truth images. Real haze from a professional haze machine was used to generate the hazy images. Each image consists of a MacBeth color checker that can be used to check the image's color response to a known state and to enhance the evaluation of the dehazing technique. Furthermore, since they are taken under restrained setting, both the hazy as well as ground truth images are shot in a similar lighting ambience. This is a significant advantage of the I-HAZE database, as it allows to objectively evaluate existing dehazing practises with conventional image quality measures like PSNR and SSIM.

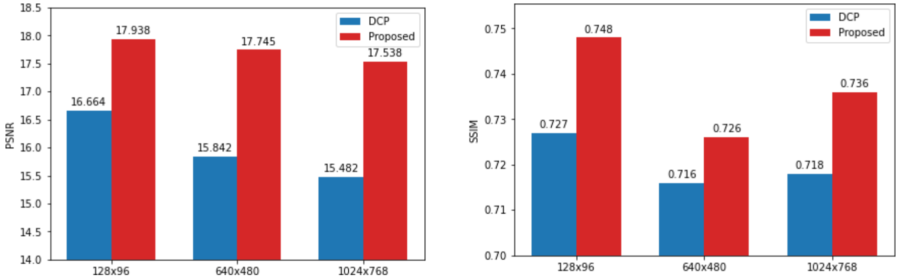

Fig. 9 PSNR and SSIM comparison of Dark Channel Prior and proposed methodology of I-HAZE Dataset

From Fig. 9 it can be perceived that for the highest resolution images, there is an increment of 2.056 dB of PSNR value by using the proposed framework. Also, it produces an increase of 0.021 in SSIM for 128×96 resolution images. which clearly shows that the proposed framework is performing well for indoor hazy images.

5.3.3 Comparison using O-HAZE Dataset

O-HAZE [30] is a haze-free outdoor scene database made up of sets of real hazy and haze-free ground truth images. Hazy images are taken in the presence of actual haze produced by the haze machines. The O-HAZE database comprises 45 distinct outdoor images portraying the identical perceptible elements captured in haze-free and hazy environments, under similar lighting constraints.

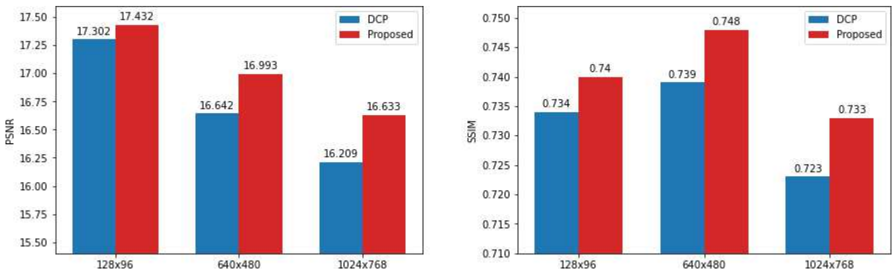

Fig. 10 PSNR and SSIM comparison of Dark Channel Prior and proposed methodology of O-HAZE Dataset

We found that while the dark channel prior-based image dehazing restores the image structure very well, but, due to inadequate airlight estimation, it produces unattractive color shifting in the hazy areas. As expected, these disruptions seem to be more prevalent in the whiter or lighter areas, where the dark channel prior generally fails. However, the proposed framework slightly improves the image quality, which results in better PSNR and SSIM (Fig. 10).

Tables 1 shows the results of applying the proposed method to the I-HAZE, O-HAZE, and D-HAZY datasets. The SSIM values obtained from He et al. (DCP) [8], Meng et al.[11], Fattal [6] and Ancuti et al. [14] for each dataset are available in [34], [35] and [30]. It can be seen that the highest SSIM for the I-HAZE dataset is obtained for Ancuti et al. which is very close to the proposed methodology. Although, the proposed methodology outshines the existing dark channel prior dehazing method. For the rest of the datasets, i.e., O-HAZE and D-HAZY (Middlebury and NYU), the proposed methodology is working well, resulting in the highest SSIM as compared to the other state-of-the-art methods. Thus, it can be inferred that the proposed methodology outperforms the competing procedures on indoor as well as outdoor images.

Table 1 Quantitative assessment of all the datasets. This table shows the average SSIM over the entire dataset.

Method	**Published Year**	**D-HAZY Middleburry [29]**	**D-HAZY NYU [36]**	**I-HAZE [35]**	**O-HAZE [30]**
He et al. [8]	2011	0.865	0.811	0.711	0.735
Meng et al. [11]	2013	0.831	0.773	0.750	0.753
Fattal [6]	2008	0.796	0.747	0.574	0.707
Ancuti et al. [14]	2013	0.829	0.771	**0.770**	0.747
Proposed	-	**0.881**	**0.842**	0.767	**0.781**

5.4 Comparison with deep learning based models

Various deep learning approaches such as CNNs and GANs are also applied in the field of image dehazing. Convolutional neural networks (CNNs) were already known to be successful in image recognition and classification applications, and thus they'd been used for image dehazing as well. For experimental purpose, we train three CNN models using indoor images dataset (I-HAZE, D-HAZY Middlebury and D-HAZY NYU) and use the outdoor images (O-HAZE dataset) for testing the accuracy. We also trained a CNN model using outdoor image dataset (O-HAZE) and tested it on indoor images (I-HAZE). The CNN model that we have used has 10 fully connected layers. Adam optimizer have been used to ensure the convergence of the model. The MSE loss function is used to train the model.

To compare the results, we also perform the dehazing task on all the indoor and outdoor datasets using two variations of Generative Adversarial Networks (GANs): Pix2Pix [37] and CycleGAN [21]. Across all the image dehazing tasks, the very same model architecture mentioned in the respective GAN papers has been used. Table 2 shows the results of applying deep learning based dehazing frameworks on the I-HAZE, O-HAZE, and D-HAZY datasets.

Table 2 Quantitative assessment of deep learning based methods. This table shows the average SSIM over the entire dataset for each model.

Model	**Training Dataset**	**SSIM**
CNN	D-HAZE Middleburry	0.551
	D-HAZE NYU	0.503
	I-HAZE	0.538
	O-HAZE	0.499
Pix2Pix GAN [37]	D-HAZE Middleburry	0.478
	D-HAZE NYU	0.461
	I-HAZE	0.501
	O-HAZE	0.481
Cycle GAN [21]	D-HAZE Middleburry	0.450
	D-HAZE NYU	0.442
	I-HAZE	0.470
	O-HAZE	0.458
Proposed methodology	D-HAZE Middleburry	**0.881**
	D-HAZE NYU	**0.842**
	I-HAZE	**0.767**
	O-HAZE	**0.781**

It can be concluded that if the model is trained on the indoor dataset and tested on the outdoor dataset, the model's accuracy is very low as compared to the proposed image dehazing method. Here, the accuracy is majorly dependent on the category of the dataset that we are using for training and testing purposes. If a model is trained on a particular type of image with specific environmental conditions and tested on another type of image having a different set of environmental conditions, we may expect a model with low accuracy. Here, we should also have an ample amount of training dataset of the same category to build a good deep learning based image dehazing model of high accuracy. Also, training a deep neural network based model like CNN or GAN takes a longer time as compared to the proposed single image dehazing technique. As it can be seen from Table 2, the highest SSIM of 0.551 is obtained for the deep learning models for the D-HAZY Middleburry dataset, which is very low as compared to the proposed single image dehazing methodology.

We also compare the SSIM of the proposed methodology with some other recent state-of-the-art deep learning based methods as well. Table 3 shows the SSIM values for various deep-learning-based dehazing methods. The methods with the greatest SSIM value are highlighted. It can be seen that the proposed methodology performs significantly better than these deep learning-based methods, which require large amounts of training data and high computing power.

5.5 Comparison with other state-of-the-art methods

To further prove the efficiency of the proposed methodology, we compare the SSIM for each image of the D-HAZY Middleburry dataset [29] with some recent state-of-the-art methods. Table 4 shows the SSIM values for various image dehazing methods. The methods that have attained the highest SSIM value

Table 3 Comparison of SSIM of state-of-the-art deep learning based methods with the proposed methodology.

Method	**Published Year**	**D-HAZY Middleburry [29]**	**D-HAZY NYU [36]**	**I-HAZE [35]**	**O-HAZE [30]**
DehazeNet [38]	2016	0.422	0.544	0.773	0.688
AOD-NET [19]	2017	0.412	0.567	0.773	0.63
DCPDN [39]	2018	0.484	0.733	**0.805**	0.732
GCANet [40]	2019	0.361	0.583	0.759	0.730
FFA - Net [41]	2019	0.452	0.691	0.794	0.733
GridNet [42]	2019	0.369	0.783	0.768	0.766
MSBDN [43]	2020	0.751	0.676	0.765	0.659
Trident [44]	2020	0.478	0.461	0.501	0.481
IDRLP [45]	2021	0.727	0.742	0.789	0.699
Proposed	-	**0.881**	**0.842**	0.767	**0.781**

are highlighted for every image. It can be seen that for most of the images in the D-HAZY Middleburry dataset, the proposed methodology has obtained the highest SSIM value. We also calculate the average SSIM over the entire dataset. It can be seen that the average SSIM obtained by CNN based image dehazing approaches such as Ren et al. [17] and Santra et al. [46] is 0.819 and 0.842, respectively. The average SSIM attained by the proposed methodology is 0.881, which is the highest as compared to other state-of-the-art methods.

5.6 Parameter Tuning

There are two parameters in the algorithm that need to be set to some constant value - Ω (constant multiplied during transmission estimation) and the patch size for dark channel computation. We tried many possible values for these parameters with our proposed method and obtained the ones producing the best results.

5.6.1 Omega (Ω)

While estimating the transmission, we introduced a parameter Ω as we don't want to completely remove the haze from our image as it may not seem natural. Hence, a small proportion of haze is kept in our method so that we may not lose the feeling of depth. The value of Ω ranges between [0,1]. In Fig. 11 we have shown the average PSNR across all the restored images along with their corresponding Ω values. To compare the two results, we used all the datasets that provide the hazy as well as ground truth images. For every value of a parameter, we run the algorithm on all the images in the dataset and computed the average PSNR across all the restored images. A higher PSNR value indicates better restoration. We can see that the best value of Ω we could get using all four datasets is between 0.90 and 0.95.

Table 4 Comparison of SSIM on D-HAZY Middlebury Dataset.

	Pierre et al.	**Berman et al.**	**Ren et al.**	**Santra et al.**	**Proposed**
Published Year	**2017 [47]**	**2016 [48]**	**2016 [17]**	**2018 [46]**	**-**
Adirondack	0.835	0.891	**0.897**	0.884	0.895
Backpack	0.901	0.842	0.879	0.85	**0.917**
Bicycle	0.678	0.841	0.938	**0.959**	0.931
Cable	0.595	0.751	0.645	0.608	**0.852**
Classroom	0.646	**0.883**	0.74	0.818	0.795
Couch	0.551	0.785	0.618	0.753	**0.821**
Flowers	0.757	**0.889**	0.783	0.814	0.795
Jadeplant	0.545	0.716	0.606	0.659	**0.82**
Mask	0.842	0.816	0.85	0.845	**0.908**
Motorcycle	0.018	0.633	0.819	0.79	**0.882**
Piano	0.643	0.814	0.715	**0.89**	0.886
Pipes	0.015	0.782	0.688	0.761	**0.831**
Playroom	0.703	0.815	0.776	0.863	**0.895**
Playtable	0.778	0.9	0.86	**0.909**	0.89
Recycle	0.904	0.925	**0.952**	0.94	0.937
Shelves	0.874	0.916	**0.944**	0.924	0.932
Shopvac	0.602	0.788	0.667	0.735	**0.817**
Sticks	0.925	0.953	**0.961**	0.93	0.948
Storage	0.769	**0.869**	0.824	0.855	0.851
Sword1	0.874	0.853	0.914	0.85	**0.917**
Sword2	0.821	**0.913**	0.885	0.881	0.9
Umbrella	0.872	**0.917**	0.909	0.903	0.888
Vintage	0.926	0.795	**0.969**	0.939	0.946
Average	0.699	0.839	0.819	0.842	**0.881**

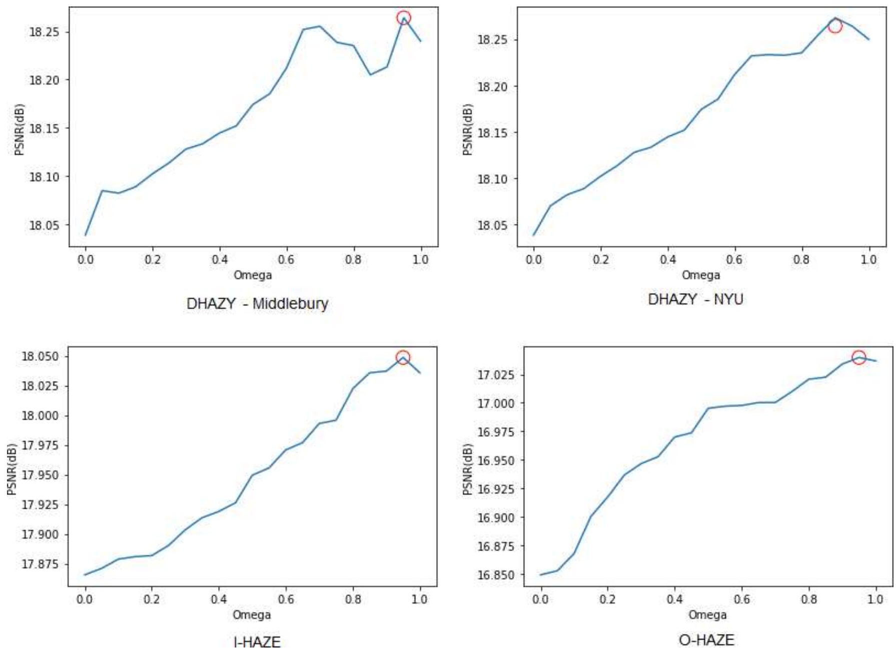

Fig. 11 Optimizing the value of Omega

5.6.2 Dark Channel Patch Size

Another critical parameter in the dehazing method is the patch size, or the window size for computing the dark channel. Fig. 12 shows resultant dehazed images obtained with various patch sizes. The restored scene radiance is seen to be over-saturated as the patch size is reduced. The colors appear over-saturated when the patch size of 3×3 is used. When a larger patch size is used, the images look more realistic. It can be inferred that the approach is effective when the patch size is reasonably large. Large patch sizes, on the other hand, can produce halos around the depth edges. In addition, the images produced by using larger patch sizes appear a bit hazier, but the variations are minor. Typically, a patch size of 15×15 is large enough to achieve acceptable results for most of the images.

In Fig. 13 we have shown the average PSNR across all the restored images along with the corresponding dark channel patch sizes. We have used all the datasets that provide the hazy as well as ground truth images. For every value of patch size, we run the algorithm on all the images in the dataset and computed the average PSNR across all the restored images. It can be seen that the best estimate of the dark channel patch size we could get using all four datasets is around 15×15.

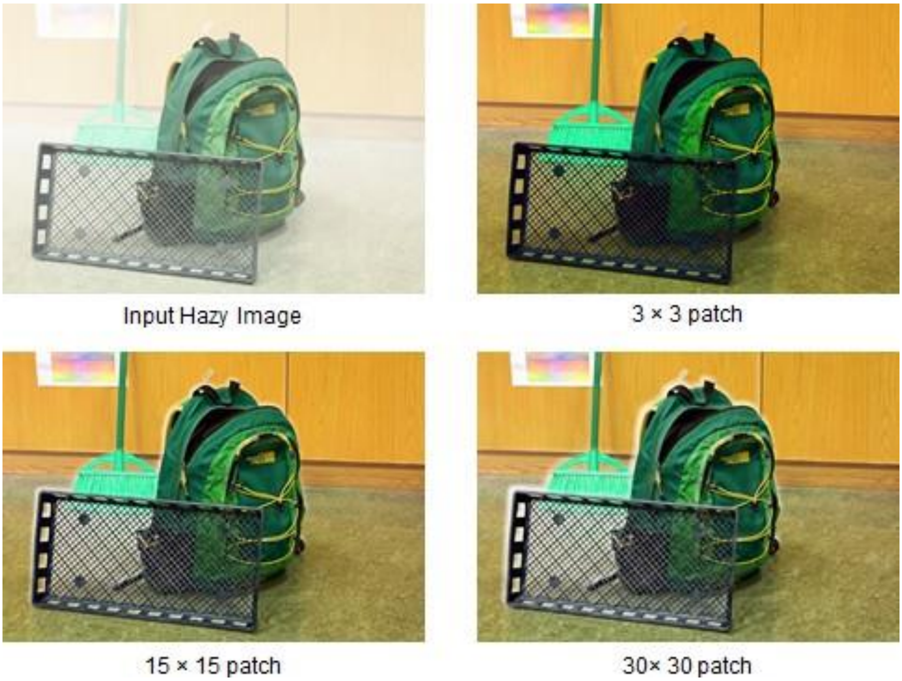

Fig. 12 Results using different path sizes

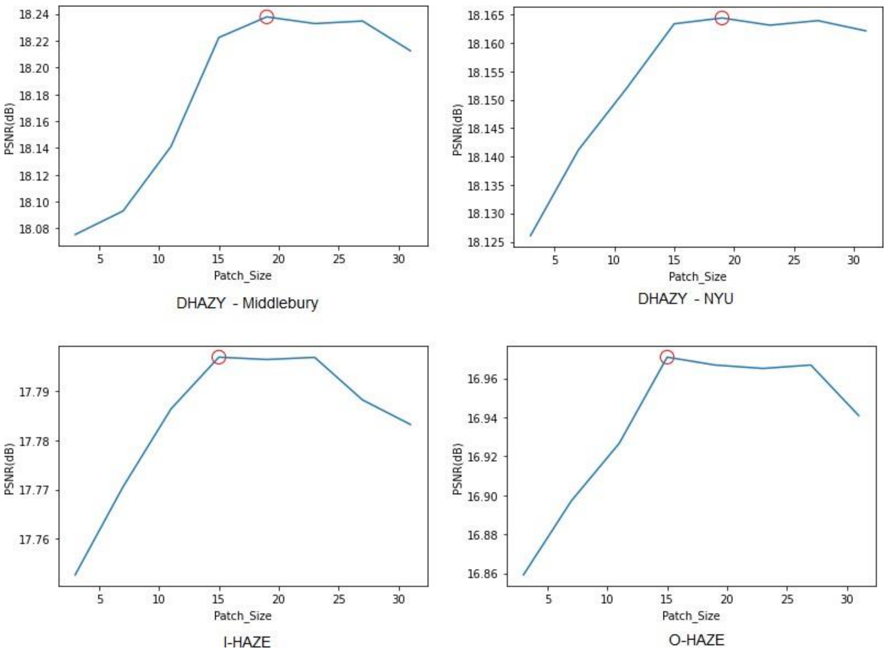

Fig. 13 Optimizing the value of dark channel path size

6 Conclusion

Natural weather environments, like haze or fog, sometimes obstruct visibility as well as the visual appeal of a scene. Thus, dehazing techniques came into existence to remove the consequences of the haze from an image. In this paper, we have extended the former technique of the existing dark channel prior to overcome the challenging issue of dehazing a hazed image. We computed the individual dark channel for each color channel of a hazy image. These individual dark channels are used to compute the transmission maps for all three color channels. The final transmission is calculated as the mean transmission, and thus, in this way, we incorporated the effect of the transmission across different channels of a hazy image. As demonstrated by numerous quality assessment experiments, the proposed approach outperforms the state-of-the-art dark channel prior image dehazing technique. The proposed methodology effectively reduces haze to a great extent and, as shown by the experiments, proves to be robust. Because the current methodology involves fine-tuning the dark channel patch size and Omega value, one of the potential future works could be to develop a more robust algorithm. The suppression of the visual artefacts of the resulting images is another factor that requires further future work. We could extend this work to eliminate haze from real-time videos as well, which could fulfil practical engineering requirements.

References

[1] Li, W.A.T.H.J.C.W. Ren, Cao: A comprehensive benchmark analysis of single image deraining: Current challenges and future perspectives. International Journal of Computer Vision **129**, 1301–1322 (2021)

[2] Garg, K., Nayar, S.K.: Vision and rain. International Journal of Computer Vision **75**, 3–27 (2007)

[3] Narasimhan, S.G., Nayar, S.K.: Vision and the atmosphere. International Journal of Computer Vision **48**, 233–254 (2002)

[4] Narasimhan, S.G., Nayar, S.K.: Chromatic framework for vision in bad weather. IEEE Conference on Computer Vision and Pattern Recognition **1**, 598–605 (2000)

[5] Tan, R.T.: Visibility in bad weather from a single image. IEEE Conference on Computer Vision and Pattern Recognition, 1–8 (2008)

[6] Fattal, R.: Single image dehazing. ACM Transactions on Graphics **27**(3), 72 (2008)

[7] McCartney, J.: Optics of the atmosphere: scattering by molecules and particles. New York, John Wiley and ons, Inc. (1976)

[8] K. He, J.S., Tang, X.: Single image haze removal using dark channel prior. IEEE Transactions on Pattern Analysis and Machine Intelligence **33**(12), 2341–2353 (2011)

[9] Chavez, P.S.: An improved dark-object subtraction technique for atmospheric scattering correction of multispectral data. Remote sensing of environment **24**, 459–479 (1988)

[10] Tarel, J., Hautiere, N.: Fast visibility restoration from a single color or gray level image. IEEE 12th International Conference on Computer Vision, 2201–2208 (2009)

[11] G. Meng, J.D.S.X. Y. Wang, Pan, C.: Efficient image dehazing with boundary constraint and contextual regularization. IEEE International Conference on Computer Vision, 617–624 (2013)

[12] Sharma, T., Verma, N.K.: Estimating depth and global atmospheric light for image dehazing using type-2 fuzzy approach. IEEE Transactions on Emerging Topics in Computational Intelligence (2020)

[13] Y. Zhang, Q.F.F.B.X.Y. P. Wang, Zhang, C.: Single image numerical iterative dehazing method based on local physical features. IEEE Transactions on Circuits and Systems for Video Technology **30**(10), 3544–3557 (2020)

[14] Ancuti, C.O., Ancuti, C.: Single image dehazing by multi-scale fusion. IEEE Transactions on Image Processing **22**(8), 3271–3282 (2013)

[15] Yin Gao, J.L. Qiming Li: Single image dehazing via a dual-fusion method. Image and Vision Computing **94** (2020)

[16] B. Cai, K.J.C.Q. X. Xu, Tao, D.: Dehazenet: an end-to-end system for single image haze removal. IEEE Transactions on Image Processing **25**(11), 5187–5198 (2016)

[17] W. Ren, H.Z.X.C.J.P. S. Liu, Yang, M.-H.: Single image dehazing via multi-scale convolutional neural networks. Proc. European Conf. Computer Vision (2016)

[18] A. Dudhane, P.W.P., Murala, S.: An end-to-end network for image dehazing and beyond. Proc. European Conf. Computer Vision (2016)

[19] B. Li, Z.W.J.X. X. Peng, Feng, D.: Aod-net: All-in-one dehazing network. IEEE International Conference on Computer Vision (ICCV), 4780–4788 (2017)

[20] Engin Deniz, E.H.K. Gen¸c Anil: Cycle-dehaze: Enhanced cycle gan for single image dehazing. Computer Vision and Pattern Recognition Workshops (2018)

[21] J. Zhu, P.I. T. Park, Efros, A.A.: Unpaired image-to-image translation using cycle-consistent adversarial networks. IEEE International Conference on Computer Vision (ICCV), 2242–2251 (2017)

[22] T. Chen, W.J.C.G. J. Fu, Liu, S.: Srktdn: Applying super resolution method to dehazing task. IEEE/CVF Conference on Computer Vision and Pattern Recognition Workshops (CVPRW), 487–496 (2021)

[23] H. Wu, Y.X.Y.Q. J. Liu, Ma, L.: Knowledge transfer dehazing network for non homogeneous dehazing. IEEE/CVF Conference on Computer Vision and Pattern Recognition Workshops (CVPRW), 1975–1983 (2020)

[24] J. Liu, Y.X.Y.Q. H. Wu, Ma, L.: Trident dehazing network. IEEE/CVF Conference on Computer Vision and Pattern Recognition Workshops (CVPRW), 1732–1741 (2020)

[25] M. Fu, Y.Y.J.C. H. Liu, Wang, K.: Dw-gan: A discrete wavelet transform gan for nonhomogeneous dehazing. IEEE/CVF Conference on Computer Vision and Pattern Recognition Workshops (CVPRW), 203–212 (2021)

[26] J. Deng, R.S.L.L.K.L. W. Dong, Fei-Fei, L.: Imagenet: A large-scale hierarchical image database. IEEE Conference on Computer Vision and Pattern Recognition, 248–255 (2009)

[27] S. -H. Gao, K.Z.X.-Y.Z.M.-H.Y. M. -M. Cheng, Torr, P.: Res2net: A new multi-scale backbone architecture. IEEE Transactions on Pattern Analysis and Machine Intelligence, 652–662 (2021)

[28] Wei Liu, G.Q. Rongguo Yao: A physics based generative adversarial network for single image defogging. Image and Vision Computing (2019)

[29] D. Scharstein, Y.K.G.K.N.N.X.W.P.W. H. Hirschmüller: High-resolution stereo datasets with subpixel-accurate ground truth. German Conference on Pattern Recognition (2014)

[30] C. O. Ancuti, R.T. C. Ancuti, Vleeschouwer, C.D.: O-haze: A dehazing benchmark with real hazy and haze-free outdoor images. IEEE/CVF Conference on Computer Vision and Pattern Recognition Workshops (CVPRW), 867–8678 (2018)

[31] Siyuan Li, F.W.I.B.A.E.K.T.R.H.J.R.M.C.-J.Z.W. Wenqi Ren, Cao, X.: Benchmarking low-light image enhancement and beyond. International Journal of Computer Vision **129**, 1258–1281 (2021)

[32] Alain Hor´e, D.Z.: Image quality metrics: Psnr vs. ssim. International Conference on Pattern Recognition (2010)

[33] Zhou Wang, H.R.S. A. C. Bovik, Simoncelli, E.P.: Image quality assessment: from error visibility to structural similarity. IEEE Transactions on Image Processing **13**(4), 600–612 (2004)

[34] C. Ancuti, C.O.A., Vleeschouwer, C.D.: D-hazy: A dataset to evaluate quantitatively dehazing algorithms. IEEE International Conference on Image Processing (ICIP), 2226–2230 (2016)

[35] Ancuti, C.O., Ancuti, C., Timofte, R., Vleeschouwer, C.D.: I-haze: a dehazing benchmark with real hazy and haze-free indoor images. ArXiv:1804.05091v1 (2018)

[36] N. Silberman, P.K.R.F. D. Hoiem: Indoor segmentation and support inference from rgbd images. European Conference on Computer Vision (2012)

[37] P. Isola, T.Z. J. Zhu, Efros, A.A.: Image-to-image translation with conditional adversarial networks. IEEE Conference on Computer Vision and Pattern Recognition (CVPR), 5967–5976 (2017)

[38] B. Cai, K.J.C.Q. X. Xu, Tao, D.: Dehazenet: An end-to-end system for single image haze removal. IEEE Transactions on Image Processing, 5187–5198 (2016)

[39] Zhang, H., Patel, V.M.: Densely connected pyramid dehazing network. IEEE/CVF Conference on Computer Vision and Pattern Recognition, 3194–3203 (2018)

[40] et al., D.C.: Gated context aggregation network for image dehazing and deraining. IEEE Winter Conference on Applications of Computer Vision (WACV), 1375–1383 (2019)

[41] Xu Qin, Y.B.X.X. Zhilin Wang, Jia, H.: Ffa-net: Feature fusion attention network for single image dehazing. arXiv preprint arXiv:1911.07559 (2019)

[42] Liu, X., Ma, Y., Shi, Z., Chen, J.: Griddehazenet: Attention-based multi-scale network for image dehazing. IEEE/CVF Int. Conf. Comput. Vis. (ICCV), 7314–7323 (2019)

[43]

[44] J. Liu, Y.X.Y.Q. H. Wu, Ma, L.: Trident dehazing network. IEEE/CVF Conference on Computer Vision and Pattern Recognition Workshops

(CVPRW), 1732–1741 (2020)

[45] Ju, M., Ding, C., Guo, C.A., Ren, W., Tao, D.: Idrlp: Image dehazing using region line prior. IEEE Transactions on Image Processing, 9043–9057 (2021)

[46] S. Santra, R.M., Chanda, B.: Learning a patch quality comparator for single image dehazing. IEEE Transactions on Image Processing **27**(9), 4598–4607 (2018)

[47] F. Pierre, A.B.G.S. J.F.Aujol, Ta, V.T.: Variational contrast enhancement of gray-scale and rgb images. Journal of Mathematical Imaging and Vision, 5967–5976 (2017)

[48] D. Berman, T.T., Avidan, S.: Non-local image dehazing. IEEE Conference on Computer Vision and Pattern Recognition (CVPR), 1674–1682 (2016)